Sérgio Luiz Waitman Filho
Faculdade de Engenharia Mecânica
Universidade Estadual de Campinas

Final Report

ES952 - Trabalho de Graduação II

Control of Lur'e Type Nonlinear Switched Systems

July 1, 2014

Universidade Estadual de Campinas
Campus Universitário Zeferino Vaz, Barão Geraldo, Campinas - SP, 13083-970

Advisor:
Profa. Dra. Grace S. Deaecto
grace@fem.unicamp.br

Advisor:
Prof. Dr. José C. Geromel
geromel@dsce.fee.unicamp.br

Abstract

This report introduces a new method for stability analysis and switching function control design of nonlinear Lur'e type switched systems. The results are based on the generalization of the describing function method. The nonlinearity is approximated by its harmonic linearization and a set of LMIs is derived for the determination of a stabilizing switching rule. On the contrary of what is needed by the celebrated circle criterion, this method does not require that the linear part of the system be asymptotically stable. However, since it is an approximation, as it occurs in the describing function method for LTI systems, this relaxation may imply the loss of sufficiency for stability, and therefore the result must be checked afterwards. Nevertheless, in this work, the validity of the procedure is verified by means of an illustrative example concerning of a mass–spring–damper with active damping.

Contents

List of Figures

Chapter 1

Introduction

The problem of absolute stability for nonlinear systems that may be represented in the so called Lur'e structure has been largely studied and many theoretical aspects have been developed since its proposition by Lur'e and Postnikov, in 1944. Since that time, several important and related results have been proven using different approaches, such as frequency domain analysis and search for a Lyapunov function candidate. See [11] for a rather complete and comprehensive review of theoretical-based developments.

On the other hand, stabilizability analysis and control design of hybrid systems appeared more recently in the literature. This area of research interest has drawn a lot of attention mainly due to its wide range of potential practical applications. The basic concepts are treated in [10] and are handled and elaborated in [9]. Many developments arose concerning stability of switched linear systems [5], switched linear systems with time delay [12] and switched Lur'e systems [3], among many others. In all these papers the stability and design conditions are expressed in terms of linear matrix inequalities which are easily handled by means of several methods available in the literature to date.

The scope of this work is to introduce switched nonlinear systems with Lur'e structure and take advantage of this particular structure to develop new analysis and design methodologies. Systems of this class are characterized by the feedback connection of a switched linear system and a time invariant nonlinearity. The main goal is to provide a control state–dependent stabilizing switching rule that is able to impose global stability. A method to find such a stabilizing switching rule based on harmonic linearization of the nonlinearity is provided. Although this method can not guarantee stability, due to the adoption of an approximation, the carried out simulations indicate that it can be a valid tool for switched nonlinear systems control design. In some sense the positive (simplicity and practical appealing) and negative (approximation) points present in the classical describing function method remain almost unchanged in this new context.

1.1 Notation

The notation used throughout this text is fairly straightforward. Matrices are represented by capital letters, whereas scalars and vectors are represented by lowercase letters. The sign ($'$) denotes the transpose of a vector or matrix. Positive definite (semidefinite) symmetric matrices are represented as $P > 0$ ($P \geq 0$). The Laplace transform of $y(t)$ defined por all $t \geq 0$ is denoted as $\widehat{y}(s) = \mathcal{L}[y(t)]$, where $s \in \mathbb{C}$ is the complex number $s = \sigma + j\omega$, for σ and ω real numbers. A square matrix is Hurwitz if all its eigenvalues are inside the left open complex plane.

Chapter 2

Key Concepts

2.1 Stability Criteria

In this section some of the classical stability criteria used in linear and nonlinear control theory are presented. This study is intended to serve as a starting point in the development of the stability analysis of the problem at hand. The first stability criterion to be presented is the well known Nyquist Criterion, proposed by the engineer Harry Nyquist when working with Bell Laboratories and applicable to linear time invariant systems. Secondly, the Lyapunov Stability Criterion, introduced by Aleksandr Lyapunov in 1892, is presented. At last, the treatment of a special category of nonlinearities is done in the context of the Lur'e Problem. Its stability analysis by means of the Circle Criterion and by the Describing Function Method is provided. With this set of stability criteria, one is able to tackle a wide range of problems among linear and nonlinear systems.

At this point, it is important to give a formal definition of the stability concept applicable to linear time-invariant (LTI) systems.

Definition 2.1 (**Stability for LTI systems**). *A linear time-invariant system with transfer function $H(s)$ and state space realization of the form $\dot{x} = Ax$ is asymptotically stable if one of the following equivalent statements is true:*

1. *The poles of $H(s)$ are located in the open left-half complex plane.*
2. *The eigenvalues of A are located in the open left-half complex plane.*
3. *$h(t) = \mathcal{L}^{-1}[H(s)] \to 0$ when $t \to \infty$.*
4. *$\int_0^t |h(\tau)|d\tau < \infty$, $\forall t \geq 0$.*

Obviously, this definition is no longer valid in the case of nonlinear systems, due to the simple fact that its transfer function can not be determined. In fact, nonlinear systems may converge to multiple isolated points in the

state space, a behaviour that is not observed in linear systems. With this in mind, in the general case, the definition of equilibrium point is now given.

Definition 2.2 (**Equilibrium point**). *Consider an autonomous unforced nonlinear system with state realization given by*

$$\dot{x} = f(x) \tag{2.1}$$

The point $x_e \in \mathbb{R}^n$ is called an equilibrium point of (2.1) if $x(0) = x_e$ implies that $x(t) = x_e, \forall t \geq 0$.

As a direct consequence of this definition, the equilibrium points are characterized by

$$\dot{x}_e = f(x_e) = 0 \tag{2.2}$$

and, consequently, the stability in the context of nonlinear systems must be verified locally for each equilibrium point. At this stage, the formal definition of equilibrium point stability may be stated.

Definition 2.3 (**Stability** [8]). *The equilibrium point $x = x_e$ of (2.1) is*

- *stable if, for each $\varepsilon > 0$, there is $\delta = \delta(\varepsilon) > 0$ such that*

$$\|x(0) - x_e\| < \delta \Rightarrow \|x(t) - x_e\| < \varepsilon, \forall t \geq 0 \tag{2.3}$$

- *unstable if it is not stable.*

- *asymptotically stable if it is stable and δ can be chosen such that*

$$\|x(0) - x_e\| < \delta \Rightarrow \lim_{t \to \infty} x(t) = x_e \tag{2.4}$$

The conditions imposed by this stability definition may be difficult to test for some class of dynamic systems because, in general, they require the formulation of parameter dependent conditions. The method proposed by Lyapunov allows stability assessment in a more simple, direct and intuitive manner.

2.1.1 Nyquist Stability Criterion

The Nyquist Stability Criterion is formulated in the frequency domain. It allows the closed–loop stability analysis of linear systems, which may or may not be open–loop stable. The analysis is based on the mapping of the system transfer function in the complex plane, the so called Nyquist Diagram. In this sense, one does not need to know the position of each and every single pole and zero of the system in question, but only the number of unstable poles (poles located in the open right-half complex plane).

In order to state the Nyquist Stability Criterion, it is important to understand an algebraic manipulation denominated Argument Principle, which is important in complex analysis and control theory (See [6] and [7] for a complete and detailed discussion on this matter). This principle is derived from the application of Cauchy's Residue Theorem to the function $f(s) : \mathbb{C} \to \mathbb{C}$ of the form

$$f(s) = \frac{g'(s)}{g(s)} \tag{2.5}$$

where $g(s) : \mathbb{C} \to \mathbb{C}$ as well. It is important to notice that the function $f(s)$ is analytic over $\mathbb{C}$, with the exception of the poles and zeros of $g(s)$. The residue of the function $f(s)$ at $s_0 \in \mathbb{C}$ is defined as being the coefficient c_{-1} of the Laurent series expansion of $f(s)$ in a neighbourhood of s_0, that is

$$f(s) = \sum_{i=-\infty}^{\infty} c_i (s - s_0)^i \tag{2.6}$$

Let us denote $R(f, s_0) = c_{-1}$. It can be shown that the residue of $f(s)$ at each pole of $g(s)$ is equal to minus its multiplicity, and at each zero of $g(s)$ it is equal to its multiplicity. Cauchy's Residue Theorem then states that

$$\begin{aligned} \frac{1}{2\pi j} \oint_{\mathcal{C}} f(s) ds &= \sum_{s_i \in \text{ int } \mathcal{C}} R(f, s_i) \\ &= N_z - N_p \end{aligned} \tag{2.7}$$

where N_z and N_p denote the number of zeros and poles of $g(s)$ enclosed by the simply connected contour $\mathcal{C}$. By noticing that the term on the left–hand side of (2.7) can be alternatively calculated as

$$\begin{aligned} \oint_{\mathcal{C}} \frac{g'(s)}{g(s)} ds &= \oint_{\mathcal{C}} d\ln(g(s)) \\ &= j \arg\left(g(s)\right)|_{\mathcal{C}} \end{aligned} \tag{2.8}$$

which can be interpreted as the variation in the argument of $g(s)$ as s travels around $\mathcal{C}$. Putting together (2.7) and (2.8), one obtain the classic statement of the Argument Principle as follows

$$\frac{1}{2\pi} \Delta_{\mathcal{C}} \arg g(s) = N_z - N_p \tag{2.9}$$

that is, the variation of the argument of $g(s)$ divided by 2π as s travels over $\mathcal{C}$ is equal to the difference between the number of zeros and poles of $g(s)$ placed inside the contour $\mathcal{C}$. The left-hand side of (2.9) represents the number of loops of the mapping of $g(s)$ over $\mathcal{C}$ around the origin.

Let us apply this result to the SISO system depicted in Figure 2.1, where $H(s)$ is the transfer function between the input $\widehat{w}(s) = \mathcal{L}[w(t)]$ and the output $\widehat{y}(s) = \mathcal{L}[y(t)]$. The Nyquist Stability Criterion is stated in Theorem 2.1.

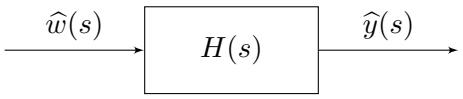

Figure 2.1: Linear system with transfer function $H(s)$

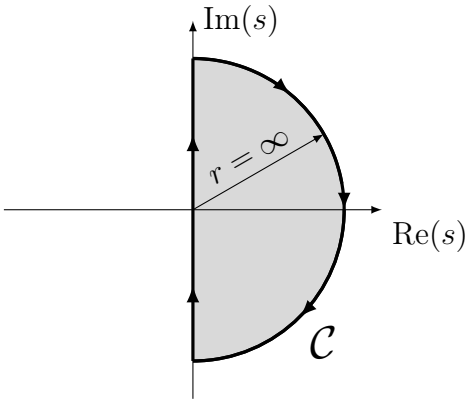

Figure 2.2: Contour $\mathcal{C}$ used in the Nyquist criterion

Theorem 2.1 (**Nyquist Stability Criterion**). *Consider a linear time invariant system with transfer function $H(s)$ and let $G(s)$ be a closed–loop transfer function of the form*

$$G(s) = \frac{\kappa H(s)}{1 + \kappa H(s)} \tag{2.10}$$

with characteristic equation $1 + \kappa H(s) = 0$. If the mapping of $H(s)$ over the contour $\mathcal{C}$ presented in Figure 2.2 is such that the number of counterclockwise encirclements around the critical point $-1/\kappa$ is equal to the number of poles of $H(s)$ inside $\mathcal{C}$ (open–loop unstable poles), then the closed–loop system transfer function $G(s)$ is asymptotically stable.

The proof is given in [6], and is repeated here for completeness. Consider the function $1+\kappa H(s)$. One can verify the validity of the Argument Principle by computing the number of turns of the mapping of $H(s)$ around the critical point $-1/\kappa$. In fact, the argument of vector $\phi(s)$ with origin at $-1/\kappa$ and extremity on $H(s)$ is given by

$$\begin{aligned} \arg\left(\phi(s)\right) &= \arg\left(H(s) + 1/\kappa\right) \\ &= \arg\left((1 + \kappa H(s))/\kappa\right) \end{aligned} \tag{2.11}$$

On the other hand, (2.11) shows that the argument variation of $\phi(s)$ is equal to the argument variation of the mapping of $1 + \kappa H(s)$ around the origin,

and consequently, this fact implies that the number of loops performed by the mapping of $H(s)$ around the critical point is equal to the number of loops performed by the mapping of $1 + \kappa H(s)$ around the origin.

Using the notation $H(s) = N(s)/D(s)$, it is possible to write

$$1 + \kappa H(s) = \frac{D(s) + \kappa N(s)}{D(s)} \tag{2.12}$$

and also

$$G(s) = \frac{\kappa N(s)}{D(s) + \kappa N(s)} \tag{2.13}$$

Hence, from (2.12) and (2.13), it can be seen that the poles of $1 + \kappa H(s)$ are the poles of the open–loop transfer function $H(s)$, and its zeros are the poles of the closed–loop transfer function $G(s)$.

Notating N_{crit} as the number of clockwise loops given by the mapping of $H(s)$ over the contour $\mathcal{C}$ presented in Figure 2.2, and applying the Argument Principle, the following relation is derived

$$N_{crit} = N_z - N_p \tag{2.14}$$

where N_z and N_p are the number of zeros of $1 + \kappa H(s)$ (poles of $G(s)$) and poles of $1 + \kappa H(s)$ (poles of $H(s)$) in the right-half complex plane, respectively. In order to assure the closed–loop system asymptotic stability, all its poles must be in the left-half complex plane, which means that $N_z = 0$. Hence, if $-N_{crit} = N_p$, that is, if the number of counterclockwise loops performed by the mapping of $H(s)$ around the critical point $-1/\kappa$ is equal to the number of open–loop unstable poles, the closed–loop system is asymptotically stable.

Special attention must be paid to the case where $H(s)$ has poles in the imaginary axis, since the contour $\mathcal{C}$ must not pass through any point where $f(s) = g'(s)/g(s)$ is not analytic, assuring that the Cauchy's Residue Theorem remains valid. In this situation, a new contour must be used, which goes around the singularities. An example of a contour that can be used when $H(s)$ presents poles at the origin is presented in Figure 2.3.

2.1.2 Lyapunov Stability Criterion

The Lyapunov Stability Criterion is a classical result largely used in the literature since its apparition, in 1892. It has been extended and applied to several and large classes of dynamic systems. It is recognized as a powerful tool for stability analysis in time domain, and a much simpler and general one when compared to other methods available in the literature.

Theorem 2.2 (**Lyapunov Stability Criterion** [8]). *Let $x_e = 0$ be an equilibrium point of* (2.1) *belonging to the domain $D \subset \mathbb{R}^n$. Let $V : \mathbb{R}^n \to \mathbb{R}$*

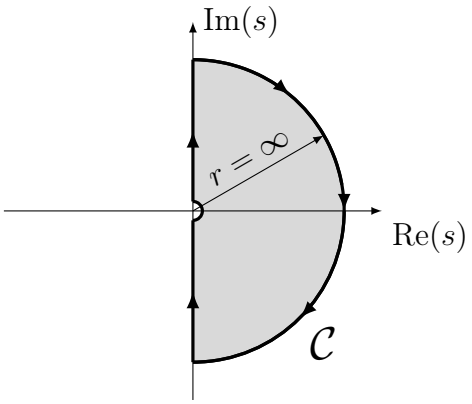

Figure 2.3: Contour $\mathcal{C}$ when $H(s)$ possesses poles at the origin

be a continuously differentiable function such that

$$V(0) = 0 \text{ and } V(x) > 0, \forall x \in D - \{0\} \tag{2.15}$$

$$\dot{V}(x) \leq 0, \forall x \in D \tag{2.16}$$

then $x_e = 0$ is stable. Moreover, if

$$\dot{V}(x) < 0, \forall x \in D \tag{2.17}$$

then $x_e = 0$ is asymptotically stable.

The proof is given in [8], and is omitted. A function $V(x)$ satisfying (2.15)–(2.16) or (2.15)–(2.17) is called a *Lyapunov function*. Theorem 2.2 allows to check for stability in a neighborhood of the equilibrium point. In order to guarantee global stability, that is, $D = \mathbb{R}^n$, a supplementary condition must be satisfied by $V(x)$, as stated in Theorem 2.3.

Theorem 2.3 (**Global Stability** [8])**.** *Let $x_e = 0$ be an equilibrium point of (2.1). Let $V : \mathbb{R}^n \to \mathbb{R}$ be a continuously differentiable function such that*

$$V(0) = 0 \text{ and } V(x) > 0, \forall x \neq 0 \tag{2.18}$$

$$\dot{V}(x) < 0, \forall x \neq 0 \tag{2.19}$$

$$\|x\| \to \infty \Rightarrow V(x) \to \infty \tag{2.20}$$

then $x_e = 0$ is globally asymptotically stable.

Again the proof is given in [8] and is omitted. The function $V(x)$ as defined in Theorem 2.3, can be seen as the distance between $x(t)$ and the origin. As $\dot{V}(x) < 0$, this distance always decreases, and $x(t) \to x_e = 0$.

Let us consider the case of an LTI system given by

$$\dot{x} = Ax \tag{2.21}$$

The function $V(x) = x'Px$, with $P \in \mathbb{R}^{n\times n}$ positive definite, is a Lyapunov function candidate and our objective is to verify if it can satisfy conditions (2.18)–(2.20). Its time derivative is given by

$$\begin{aligned}\dot{V}(x) &= \dot{x}'Px + x'P\dot{x} \\ &= (Ax)'Px + x'P(Ax) \\ &= x'(A'P + PA)x \end{aligned} \tag{2.22}$$

Given $Q \in \mathbb{R}^{n\times n}$ a positive semidefinite matrix, if it is possible to find $P > 0$ such that

$$A'P + PA = -Q \tag{2.23}$$

the relation given in (2.22) becomes

$$\begin{aligned}\dot{V}(x) &= -x'Qx \\ &< 0, \quad \forall x \neq 0 \end{aligned} \tag{2.24}$$

It can be shown that the Lyapunov matrix equation (2.23) is solvable with respect to $P > 0$ if and only if the unique equilibrium point $x_e = 0$ of the linear time invariant system (2.21) is asymptotically stable [6].

2.1.3 Lur'e Problem

The so called Lur'e Problem of Absolute Stability was introduced by Lur'e and Postnikov in 1944. It concerns systems that exhibit the following state space realization

$$\dot{x} = Ax + Bw \tag{2.25}$$
$$y = Cx + Dw \tag{2.26}$$
$$e = r - y \tag{2.27}$$
$$w = \phi(e) \tag{2.28}$$

where $x(t) \in \mathbb{R}^n$ is the state and $y, r, e, w \in \mathbb{R}$ are the output, the reference, the error and the input signal, respectively. The related block diagram is given in Figure 2.4. To ease the presentation and because the main aspects of the stability analysis remain present we assume the linear part of the system has a strictly proper transfer function $H(s) = C(sI - A)^{-1}B$ which implies that $D = 0$. The general case $D \neq 0$ can be considered but at the expense of increasing the involved algebraic manipulations.

The function $\phi : \mathbb{R} \to \mathbb{R}$ is nonlinear, memoryless and locally Lipschitz. Additionally, it is assumed that $\phi(\cdot)$ is such that

$$\kappa_1 e^2 \leq e\phi(e) \leq \kappa_2 e^2, \quad 0 \leq \kappa_1 \leq \kappa_2 \in \mathbb{R} \tag{2.29}$$

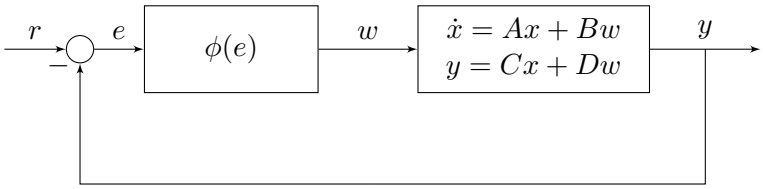

Figure 2.4: Lur'e system structure

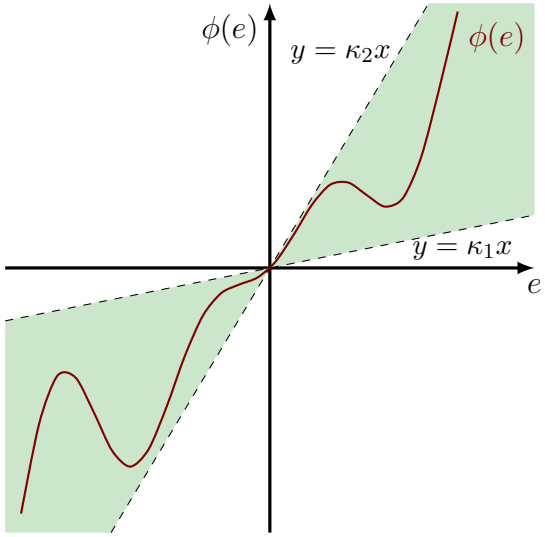

Figure 2.5: The nonlinear function $\phi(e)$ in the sector $[\kappa_1, \kappa_2]$

This is equivalent to say that $\phi(e)$ is contained in the region between the straight lines $y = \kappa_1 x$ and $y = \kappa_2 x$, as illustrated in Figure 2.5. We then say that $\phi(\cdot)$ belongs to sector $[\kappa_1, \kappa_2]$ [8]. As a consequence of this property, the function is such that $\phi(0) = 0$. For any $\phi(\cdot)$ belonging to the sector $[\kappa_1, \kappa_2]$, $x_e = 0$ is an equilibrium point of the nonlinear system (2.25)–(2.28).

The problem of absolute stability consists in finding sufficient conditions under which the origin is a globally asymptotically stable equilibrium point. This problem has been largely treated in the literature [11], and some classical results are given in Sections 2.1.3.1 and 2.1.3.2.

An interesting problem regarding this class of systems was formulated by Aizerman [1] (in Russian; see [11] for a discussion in English), and became known as *Aizerman's conjecture*. Let us consider the function

$$\phi(e) = \kappa e, \quad \kappa \in [\kappa_1, \kappa_2] \tag{2.30}$$

If the system represented by (2.25)–(2.28) with $\phi(e)$ given by (2.30) is proven to be asymptotically stable, does it follow that (2.25)–(2.28) with $\phi(e)$ non-

linear is absolutely stable? This conjecture was proven to be false, and gave rise to other conjectures with more rigid conditions on $\phi(e)$, which ended proven false as well [11]. These theoretical efforts and discussions indicate the important result that absolute stability requires the fulfilment of more stringent conditions than the linear case.

2.1.3.1 Circle Criterion

The Circle Criterion gives sufficient conditions under which the system (2.25)–(2.28) is absolutely stable. Prior to its statement, it is important to introduce some new concepts. Firstly, the passivity property is addressed, as well as the frequency domain counterpart.

A motivation for the concept of passivity can be found in electric networks [8]. A one-port resistive element is passive if the inflow of power is always nonnegative. If the voltage $w(t)$ is the input, and the current $y(t)$ is the output, the power flowing through the device is $p(t) = y(t)w(t)$. For the resistive element to be passive, $p(t) \geq 0$, which means that the voltage-current curve must lie in the first and third quadrants. A formal definition of passivity is given below.

Definition 2.4 (**Passivity** [8]). *The system*

$$\dot{x} = f(x, w) \tag{2.31}$$
$$y = h(x, w) \tag{2.32}$$

where $x(t) : \mathbb{R}_+ \to \mathbb{R}^n$, $x(0) = 0$ *and* $y(t) : \mathbb{R}_+ \to \mathbb{R}^p$, $w(t) : \mathbb{R}_+ \to \mathbb{R}^p$ *is* passive *if there exists a continuously differentiable positive semidefinite function* $V(x)$ *(called the storage function) such that*

$$y'w \geq \dot{V}(x) \ \forall w \in \mathbb{R}^p \tag{2.33}$$

Choosing $V(x)$ as a Lyapunov function, and integrating both sides of (2.33) from $t = 0$ to $t \to \infty$, one obtains

$$\begin{aligned} \int_0^\infty y(t)'w(t)dt &\geq V(x(\infty)) - V(x(0)) \\ &\geq 0 \end{aligned} \tag{2.34}$$

which is another way to formulate the passivity condition. Since passivity is independent of the input, from (2.33) with $w \equiv 0$, and considering the strict inequality, we obtain $\dot{V}(x) < 0$ which shows that global asymptotic stability is a necessary condition for strict passivity.

For simplicity, from now on only the scalar case characterized by $p = 1$ (scalar input and output) will be treated. The concept of passivity has a

counterpart in the frequency domain. Indeed, applying Parseval's Theorem to (2.34) gives

$$\begin{aligned}\int_0^\infty y(t)w(t)dt &= \frac{1}{2\pi}\int_{-\infty}^{\infty}\widehat{y}(j\omega)\widehat{w}(-j\omega)d\omega \\ &= \frac{1}{2\pi}\int_{-\infty}^{\infty}H(j\omega)|\widehat{w}(j\omega)|^2dw \\ &= \frac{1}{\pi}\int_0^\infty \mathrm{Re}\left(H(j\omega)\right)|\widehat{w}(j\omega)|^2dw \end{aligned} \tag{2.35}$$

As (2.35) must hold for any arbitrary input $w(t)$, it implies that the transfer function of a passive system is contained in the right-half complex plane. A transfer function $H(s)$ with this property is called *positive real*.

Definition 2.5 (**Positive Realness** [6]). *The transfer function $H(s) : \mathbb{C} \to \mathbb{C}$ is positive real if it is Hurwitz stable and*

$$Re(H(j\omega)) \geq 0, \forall\omega \in \mathbb{R} \tag{2.36}$$

If the inequality is strict, $H(s)$ is called strictly positive real.

It can be shown that the negative feedback connection of two strictly passive systems is also strictly passive [8], and hence globally asymptotically stable. With this result, it can be proven that system (2.25)-(2.28) is globally asymptotically stable if $H(s) = C(sI - A)^{-1}B + D$ is strictly positive real and $\phi(e)$ belongs to sector $[0, \infty]$ [6].

The sector condition on $\phi(e)$ may be too conservative. Some nonlinear functions can be contained in a smaller sector $[\kappa_1, \kappa_2]$, as already discussed. This "excess of passivity" of $\phi(e)$ allows $H(s)$ to be "less passive". This idea is behind the so called Circle Criterion, stated below.

Theorem 2.4 (**Circle Criterion** [8]). *The system* (2.25)–(2.28) *is absolutely stable if $\phi(e) \in [\kappa_1, \kappa_2]$ and*

$$\mathcal{Z}(s) = \frac{1 + \kappa_2 H(s)}{1 + \kappa_1 H(s)} \tag{2.37}$$

is strictly positive real.

The proof comes from the analysis of the Nyquist plot of $\mathcal{Z}(j\omega)$, and is given in [8]. The complex numbers $1 + \kappa_2 H(j\omega)$ and $1 + \kappa_1 H(j\omega)$ are represented by the lines connecting $H(j\omega)$ to $-1/\kappa_2$ and $-1/\kappa_1$, respectively. This can be seen in Figure 2.6. The ratio in $\mathcal{Z}(j\omega)$ has positive real part if $|\theta_1 - \theta_2| < \pi/2$, which is true as long as $H(j\omega)$ does not enter in the circle passing through the points $-1/\kappa_1$ and $-1/\kappa_2$. Also, the condition $\mathcal{Z}(j\omega)$ Hurwitz stable is equivalent to $\kappa_1 H(j\omega)/(1 + \kappa_1 H(j\omega))$ Hurwitz stable as well. As seen in Section 2.1.1, this is met if the Nyquist plot of $H(s)$ encircles

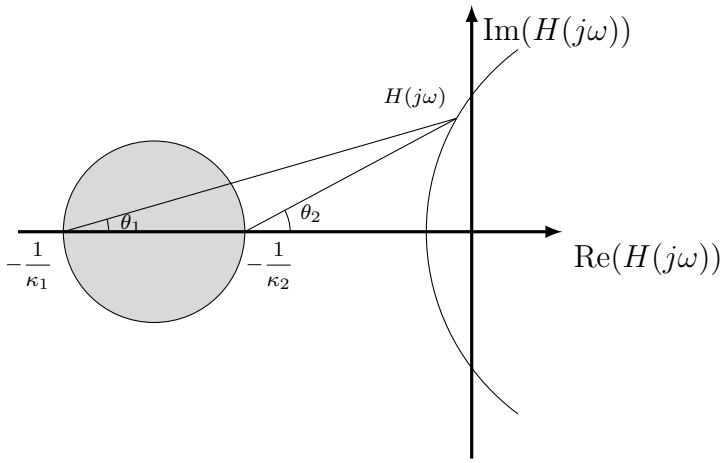

Figure 2.6: Graphical representation of the circle criterion [8]

the critical point $-1/\kappa_1$ in the counterclockwise direction a number of times equal to the number of unstable poles in $H(s)$.

There is another way to interpret geometrically the condition assuring that $\mathcal{Z}(s)$ is strictly positive real. Indeed, to ease the notation, for each $\omega \in \mathbb{R}$, let us set $\mathrm{Re}(H(j\omega)) = \sigma$ and $\mathrm{Im}(H(j\omega)) = \upsilon$ and verify that $\mathrm{Re}(\mathcal{Z}(j\omega)) > 0$ can be written as

$$1 + (\kappa_1 + \kappa_2)\sigma + \kappa_1\kappa_2\sigma^2 + \kappa_1\kappa_2\upsilon^2 > 0 \tag{2.38}$$

which after some tedious but simple algebraic manipulations can be factorized as

$$\left(\sigma + \frac{\kappa_1 + \kappa_2}{2\kappa_1\kappa_2}\right)^2 + \upsilon^2 > \left(\frac{\kappa_1 - \kappa_2}{2\kappa_1\kappa_2}\right)^2 \tag{2.39}$$

This inequality defines exactly the region outside the circle indicated in Figure 2.6 and clearly justifies the name Circle Criterion.

If $\phi(e)$ belongs to sector $[0, \kappa]$, the circle degenerates to a rectangular region. Actually, fixing $\kappa_2 = \kappa$ and making $\kappa_1 \to 0$, the radius of the circle in Figure 2.6 tends to infinity. In this case, system (2.25)–(2.28) is absolutely stable if

$$\mathrm{Re}\,(H(j\omega)) > -1/\kappa, \;\; \forall\omega \in \mathbb{R} \tag{2.40}$$

2.1.3.2 Harmonic Linearization

The system (2.25)–(2.28) may present a periodic solution

$$y(t+T) = y(t), \;\; \forall t \geq 0 \tag{2.41}$$

The Harmonic Linearization method provides a tool for finding such solutions in Lur'e type systems. It relies on the approximation of $\phi(e)$ by the so called describing function $L_\phi(a)$.

Consider $r(t) \equiv 0$, and $y(t) = a\sin(\omega t)$ is a periodic solution of the system (2.25)-(2.28). Hence, the memoryless function $\phi(e)$ provides $w(t) = \phi(-y) = \phi(-a\sin(\omega t))$ which is periodic with period T. Notice that we may ignore the minus sign, as the goal is only to verify the existence of periodic solutions, and not to calculate its amplitude and phase. The idea is that the period of the solution is characterized by the fundamental frequency of $y(t)$, that is, the first term in the Fourier expansion of $w(t)$

$$w(t) \approx \alpha\sin(\omega t) + \beta\cos(\omega t) \tag{2.42}$$

where it is assumed that the offset is zero, and α and β are given by

$$\alpha = \frac{1}{\pi}\int_{-\pi}^{\pi} \phi(a\sin(\theta))\sin(\theta)d\theta \tag{2.43}$$

$$\beta = \frac{1}{\pi}\int_{-\pi}^{\pi} \phi(a\sin(\theta))\cos(\theta)d\theta \tag{2.44}$$

The describing function is defined as follows.

Definition 2.6 (**Describing Function** [6]). *Consider $\phi(e) : \mathbb{R} \to \mathbb{R}$ a real variable function. The complex valued function $L_\phi(a) : a > 0 \to \mathbb{C}$ given by*

$$L_\phi(a) = \frac{\alpha + j\beta}{a} \tag{2.45}$$

is the describing function associated to $\phi(e)$.

Let us consider the open–loop system depicted in Figure 2.1. If $H(s)$ is asymptotically stable, the response in steady state to the input $w(t) = a\sin(\omega t)$ is

$$\begin{aligned} y(t) &= a|H(j\omega)|\sin(\omega t + \angle H(j\omega) \\ &= a\,\mathrm{Re}(H(j\omega))\sin(\omega t) + a\,\mathrm{Im}(H(j\omega))\cos(\omega t) \end{aligned} \tag{2.46}$$

Putting together (2.45) and (2.46), one finally obtain

$$\begin{aligned} L_H(a) &= \frac{a\,\mathrm{Re}(H(j\omega)) + ja\,\mathrm{Im}(H(j\omega))}{a} \\ &= H(j\omega) \end{aligned} \tag{2.47}$$

With this result, it becomes clear that the describing function associated with a nonlinear function may be interpreted as a transfer function but notice that this is only an approximation. It is then possible to replace $\phi(e)$ in (2.25)–(2.28) by its describing function, as shown in Figure 2.7. As discussed in Section 2.1.1, the stability of the linear system given in Figure 2.7 may be analyzed by means of the Nyquist Criterion applied to the characteristic equation $1 + L_\phi(a)H(s)$. In this case, the critical point is in fact a critical

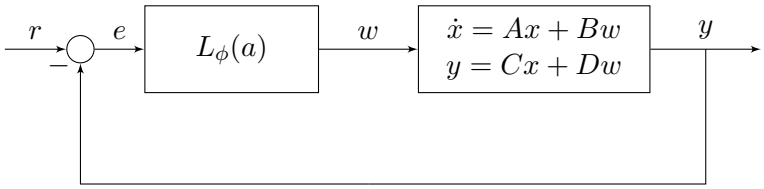

Figure 2.7: Generalized Lur'e structure

region, given by $-L_\phi(a)^{-1}$, $\forall a > 0$. Let us consider the intersection points, that is, the points (a_c, ω_c) for which $-L_\phi(a_c) = H(j\omega_c)$. These points have the properties $|L_\phi(a_c)||H(j\omega_c)| = 1$ and $\angle L_\phi(a_c) + \angle H(j\omega_c) = -\pi$. Let us admit the existence of a periodic solution $y(t) = a_c \sin(\omega_c t + \varphi)$. According to Figure 2.7, with $r(t) \equiv 0$, $y(t)$ is such that

$$\begin{aligned} y(t) &= -a_c|L_\phi(a_c)||H(j\omega_c)| \sin(\omega_c t + \varphi + \angle L_\phi(a_c) + \angle H(j\omega_c)) \\ &= a_c|L_\phi(a_c)||H(j\omega_c)| \sin(\omega_c t + \varphi + \angle L_\phi(a_c) + \angle H(j\omega_c) + \pi) \\ &= a_c \sin(\omega_c t + \varphi) \end{aligned} \tag{2.48}$$

The periodic solution hypothesis is hence consistent, and $y(t)$ is an approximation to the exact solution to (2.25)–(2.28). The stability of the limit cycle whose first harmonic approximation is $y(t)$ can be analyzed through the Nyquist Criterion, as will be detailed in Example 2.1.

Example 2.1. Consider a linear system with transfer function given by

$$H(s) = \frac{1}{s(s+2)(s+5)} \tag{2.49}$$

The goal is to verify the existence of a periodic solution when the loop is closed with a saturation on the feedback channel, that is

$$\phi(e) = \begin{cases} h & e > \frac{h}{\kappa} \\ \kappa e & |e| \leq \frac{h}{\kappa} \\ -h & e < -\frac{h}{\kappa} \end{cases} \tag{2.50}$$

Due to the fact that $\phi(e)$ is odd, the term β in (2.45) is zero, and $L_\phi(a)$ is real. The describing function is given by

$$L_\phi(a) = \begin{cases} \kappa & , 0 < a \leq \dfrac{h}{\kappa} \\ \dfrac{2\kappa}{\pi} \sin^{-1}\left(\dfrac{h}{\kappa a}\right) + \dfrac{2h}{\pi a^2}\sqrt{a^2 - \left(\dfrac{h}{\kappa}\right)^2} & , \dfrac{h}{\kappa} < a \end{cases} \tag{2.51}$$

which is depicted in Figure 2.8 for the normalized case $\kappa = h = 1$. It may be

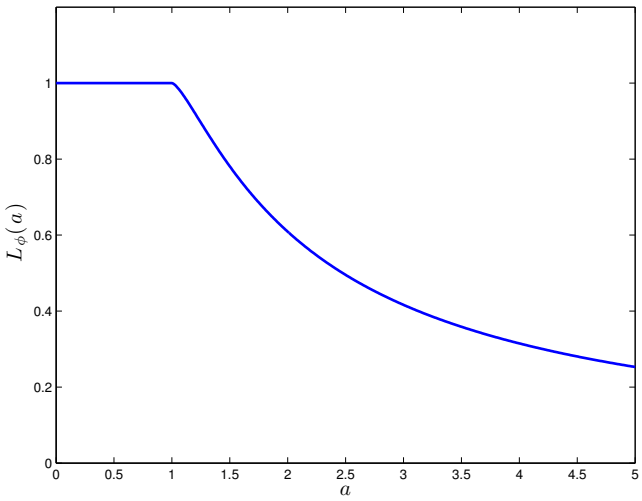

Figure 2.8: Describing function $L_\phi(a)$ for the saturation

noted that $L_\phi(a)$ decreases as a increases, whenever the effect of saturation becomes more representative. The critical region is a straight line over the $\mathrm{Re}(s)$ axis, corresponding to $-L_\phi(a)^{-1} \in \mathbb{R}$. Through analysis of $-L_\phi(a)^{-1}$, it is immediate to verify that its maximum occurs in the interval $0 < a \leq h/\kappa$, and is equal to $-1/\kappa$. The Nyquist plot of $H(s)$, presented in Figure 2.9, indicates that there is an intersection between the mapping of $H(j\omega)$ and the critical region only for κ greater than a certain value. Calculating the frequencies in which the mapping of $H(j\omega)$ crosses the real axis, one obtain $\omega_c = \pm\sqrt{10}$ and $\omega_c \to \infty$. Solving the equation $-1/\kappa = \mathrm{Re}(H(j\omega_c))$, we determine $\kappa_c = 70$. Using $\kappa = 1.5\kappa_c$, the equation $-L_g(a_c)^{-1} = H(j\omega_c)$ yields $(a_c, \omega_c) = (1.8074, 3.1623)$.

This result has been validated by time simulation performed with numerical facilities provided by SIMULINK, where both the nonlinear and linear systems were implemented. Under given initial conditions, the curves in Figure 2.10 were obtained, making clear the existence of a limit cycle with amplitude $a_c \approx 1.83$ and oscillation frequency $\omega_c \approx \pi$ rad/s in both systems. It is important to emphasize that the approximation given by the harmonic linearization method allows to draw relevant and precise conclusions about the real system under consideration.

2.2 Switched Systems

There are two main classes of dynamic systems which are characterized by the nature of the independent variable, namely continuous-time and discrete-

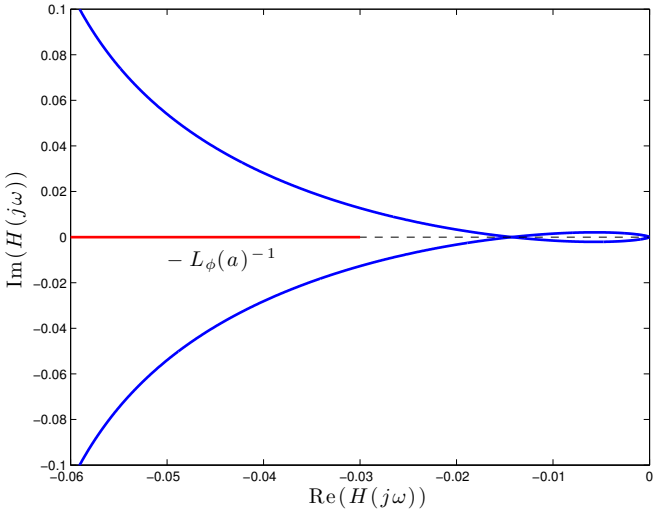

Figure 2.9: Nyquist plot of $H(s)$

time. In recent years, however, a new class of systems has drawn significant attention from the scientific community: hybrid systems. As the name suggests, hybrid systems exhibit a behavior that is an interaction between continuous evolution and discrete-time events. A classical example, taken from [9], is that of a simplified model of an automobile given by

$$\dot{x}_1 = x_2 \tag{2.52}$$

$$\dot{x}_2 = f(a, q) \tag{2.53}$$

where the states x_1 and x_2 are the position and the velocity, respectively, $a \geq 0$ is the acceleration input and $q \in \{1, 2, 3, 4, 5, 0, -1\}$ is the gear shift position. In this system, (x_1, x_2) are continuous states and q is a discrete one, and it is clear that the trajectories of the system are influenced by the transitions imposed by q.

There are different classes of hybrid systems, but the study presented here focus on linear systems with controlled state–dependent switching. This kind of systems are denominated *switched linear systems* and are represented by

$$\dot{x}(t) = A_{\sigma(t)}x(t), \quad x(0) = x_0 \tag{2.54}$$

where $x \in \mathbb{R}^n$ is the state vector, $\sigma(t) = g(x(t)) : t \geq 0 \to \mathbb{K} := \{1, 2, \ldots, N\}$ is a state–dependent switching function that selects one matrix $A_{\sigma(t)} \in \{A_1, \ldots, A_N\} \subset \mathbb{R}^{n\times n}$ at each instant of time $t \geq 0$. The approach that follows is based on the results stated in [2].

The interest lies in determining $\sigma(t)$ such that system (2.54) is globally asymptotically stable. If $\{A_1, \ldots, A_N\}$ contains at least one Hurwitz

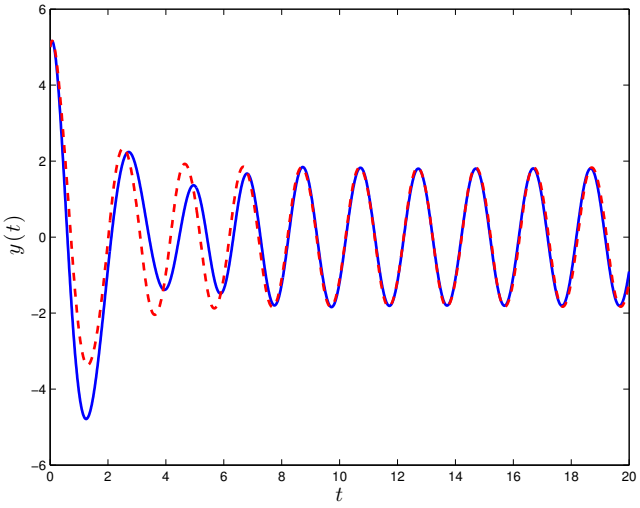

Figure 2.10: Time simulation of nonlinear and linear systems

matrix, the solution is trivial as $\sigma(t) \equiv i$, for some $i \in \mathbb{K}$ such that A_i is Hurwitz, guarantees global asymptotic stability. Nevertheless, it might still be interesting to consider switching control, as it can be shown that, under some conditions, the performance of the switched system (2.54) is guaranteed to be better than that of each isolated subsystem [4]. In summary, it is important to design a switching rule that works well in all situations.

Consider the piecewise quadratic Lyapunov function

$$V(x) = \min_{i \in \mathbb{K}} x' P_i x = \min_{\lambda \in \Lambda} \left(\sum_{i=1}^{N} \lambda_i x' P_i x \right) \tag{2.55}$$

where $\{P_1, \ldots, P_N\} \subset \mathbb{R}^{n \times n}$ are symmetric positive definite matrices and $\lambda \in \mathbb{R}^N$ belongs to the convex set

$$\Lambda = \left\{ \lambda \in \mathbb{R}^N : \sum_{i=1}^{N} \lambda_i = 1, \lambda_i \geq 0 \right\} \tag{2.56}$$

The following theorem may be stated. It provides design conditions for the determination of a stabilizing switching state–dependent function.

Theorem 2.5 (Switching function design [5])**.** *Assume that there exist a set* $\{P_1, \ldots, P_N\}$ *of positive definite matrices and a scalar* $\gamma > 0$ *satisfying the modified Lyapunov–Metzler inequalities*

$$A_i' P_i + P_i A_i + \gamma (P_j - P_i) < 0, \quad i \neq j \in \mathbb{K} \tag{2.57}$$

The state–dependent switching function $\sigma(t) = g(x(t))$ *with*

$$g(x(t)) = \arg\min_{i \in \mathbb{K}} x(t)' P_i x(t) \tag{2.58}$$

makes the equilibrium solution $x_e = 0$ *of* (2.54) *globally asymptotically stable.*

The proof is given in [5], and is omitted here. It can be shown that for (2.57) be feasible, the set $\{A_1, \ldots, A_N\}$ must admit an asymptotic stable convex combination $A_{\lambda_0} = \sum_{i=1}^{N} \lambda_{0i} A_i$, for some $\lambda_0 \in \Lambda$. Moreover, it is important to notice that the inequality (2.57) is nonconvex and, consequently, can not be handled by LMI solvers. This difficulty can be circumvented by noticing that the optimal $\gamma > 0$ may be found by line search through the minimization of a pre-specified objective function, see [5].

Chapter 3

Lur'e Type Switched Systems

3.1 Problem Definition

In this section, the problem to be studied is formally stated, with the aid of the concepts introduced in Chapter 2. Consider the closed–loop system with a generalized Lur'e structure, that is

$$\dot{x} = A_{\sigma(t)}x + Bw \tag{3.1}$$
$$y = Cx \tag{3.2}$$
$$e = r - y \tag{3.3}$$
$$w = \phi(e) \tag{3.4}$$

where $x(t) \in \mathbb{R}^n$ is the state vector and $y, r, e, w \in \mathbb{R}$ are the output, the reference, the error and the input signals, respectively. The nonlinearity $\phi : \mathbb{R} \to \mathbb{R}$ is memoryless, locally Lipschitz and we assume that $\phi(0) = 0$ which implies that the origin $x_e = 0$ is an equilibrium point whenever $r = 0$. The state-dependent switching function is of the form $\sigma(t) = g(x(t)) : t \geq 0 \to \mathbb{K}$, where $\mathbb{K} = \{1, \ldots, N\}$ and selects a linear subsystem defined by matrices

$$\mathcal{G}_i = \begin{bmatrix} A_i & B \\ C & 0 \end{bmatrix} \quad , \forall i \in \mathbb{K} \tag{3.5}$$

at each time $t \geq 0$. The goal is to design $g(x) : \mathbb{R}^n \to \mathbb{K}$ in such a way that the closed–loop switched system governed by $\sigma(t) = g(x(t))$ is asymptotically stable.

3.2 Stability

A generalization of the circle criterion providing sufficient conditions for global asymptotic stability has been given in [3]. Let us consider system (3.1)–(3.4) with null reference $r(t) \equiv 0$. Using the quadratic Lyapunov function

candidate $V(x) = x'Px$, with $P > 0$, one can readily determine

$$\begin{aligned}\dot{V}(x) &= \dot{x}'Px + x'P\dot{x} \\ &= (A_{\sigma(t)}x + Bw)'Px + x'P(A_{\sigma(t)}x + Bw)\end{aligned} \tag{3.6}$$

and choosing a switching function that minimizes (3.6), that is

$$\begin{aligned}\sigma(x) &= \arg\min_{i\in\mathbb{K}} \dot{V}(x) \\ &= \arg\min_{i\in\mathbb{K}} x'(A_i'P + PA_i)x\end{aligned} \tag{3.7}$$

the time derivative of the Lyapunov function (3.6) becomes

$$\begin{aligned}\dot{V}(x) &= \min_{i\in\mathbb{K}}(A_ix + Bw)'Px + x'P(A_ix + Bw) \\ &= \min_{\lambda\in\Lambda}(A_\lambda x + Bw)'Px + x'P(A_\lambda x + Bw) \\ &\leq (A_{\lambda_0}x + Bw)'Px + x'P(A_{\lambda_0}x + Bw) \\ &\leq \begin{bmatrix}x\\w\end{bmatrix}' \begin{bmatrix}A_{\lambda_0}'P + PA_{\lambda_0} & PB \\ B'P & 0\end{bmatrix} \begin{bmatrix}x\\w\end{bmatrix} \\ &\leq \begin{bmatrix}x\\w\end{bmatrix}' \begin{bmatrix}A_{\lambda_0}'P + PA_{\lambda_0} & PB - \kappa C'\\ B'P - \kappa C & -2I\end{bmatrix} \begin{bmatrix}x\\w\end{bmatrix} + \begin{bmatrix}x\\w\end{bmatrix}' \begin{bmatrix}0 & \kappa C'\\ \kappa C & 2I\end{bmatrix} \begin{bmatrix}x\\w\end{bmatrix}\end{aligned} \tag{3.8}$$

where the first inequality follows from any $\lambda_0 \in \Lambda$. Moreover, if there exists $P > 0$ such that the linear matrix inequality

$$\begin{bmatrix}A_{\lambda_0}'P + PA_{\lambda_0} & PB - \kappa C'\\ B'P - \kappa C & -2I\end{bmatrix} < 0 \tag{3.9}$$

is satisfied, then (3.8) becomes

$$\begin{aligned}\dot{V}(x) &< \begin{bmatrix}x\\w\end{bmatrix}' \begin{bmatrix}0 & \kappa C'\\ \kappa C & 2I\end{bmatrix} \begin{bmatrix}x\\w\end{bmatrix} \\ &< \kappa w'Cx + \kappa x'C'w + 2w'w\end{aligned} \tag{3.10}$$

Finally, taking into account the following relations $y = Cx$ and $w = \phi(-y) \in [-\kappa, 0]$, this inequality implies that

$$\begin{aligned}\dot{V}(x) &< 2(w + \kappa y)w \\ &< 2\Big(\phi(-y) + \kappa y\Big)\phi(-y) \\ &< 0\end{aligned} \tag{3.11}$$

as long as $-\phi(-y) \in [0, \kappa]$. This result generalizes the circle criterion discussed in Section 2.1.3.1 to the case of switched linear systems. It allows

the design of the switching function (3.7) which assures the origin $x_e = 0$ is a global asymptotic stable equilibrium point of the switched linear system under consideration.

The LMI (3.9) is feasible with respect to $P > 0$ only if A_{λ_0} is Hurwitz stable. It is important to notice that this result is compatible with the statements of the circle criterion. In fact, if the linear system in (2.25)–(2.28) is unstable, the mapping of its transfer function $H(s)$ must encircle the critical point $-1/\kappa_1$ a number of times equal to the unstable poles. As $\kappa_1 \to 0$, the critical point is shifted to $-\infty$. In this case, $H(s)$ must be such that $\mathrm{Re}(H(j\omega)) > -1/\kappa$, and hence cannot encircle the critical point which imposes A_{λ_0} Hurwitz stable.

In this work our purpose is to use a different approach. Actually, applying the harmonic linearization the nonlinearity $\phi(e)$ is approximated by its describing function $L_\phi(a)$. The goal is to find a switching rule able to stabilize (3.1)–(3.4) even when system (3.5) does not admit a Hurwitz stable convex combination A_λ.

To this end, the closed–loop system in (3.1)–(3.4) is given by

$$\dot{x} = \Big(A_{\sigma(t)} + B\phi(-Cx)\Big)x \tag{3.12}$$

$$y = Cx \tag{3.13}$$

and $\phi(e)/e$ is approximated by $L_\phi(a) \in \mathbb{R}$ which is always true whenever $\phi(e)$ is odd, hence $\beta = 0$ in (2.45) and $L_\phi(a)$ is a scalar positive real number. The describing function method depends crucially on the points where $-L_\phi(a)^{-1}$ intersects the mapping of $H(i\omega)$. The occurrence of such points depends on the maximum of $-L_\phi(a)^{-1}$, that is denoting

$$-\frac{1}{\bar{\kappa}} = \sup_{a\in\mathbb{R}^+} -\frac{1}{L_\phi(a)} \tag{3.14}$$

then we have to determine a stabilizing switching function for the uncertain switched linear system

$$\dot{x} = (A_{\sigma(t)} - \kappa BC)x \tag{3.15}$$

$$y = Cx \tag{3.16}$$

for all $\kappa \in (0, \bar{\kappa}]$. For stability analysis, let us consider the quadratic Lyapunov function candidate $V(x) = x'Px$ where $P > 0$. Its time derivative is given by

$$\dot{V}(x) = x'\Big((A_{\sigma(t)} - \kappa BC)'P + P(A_{\sigma(t)} - \kappa BC)\Big)x \tag{3.17}$$

and if we choose $\sigma(x)$ that minimizes the derivative of the Lyapunov function, that is

$$\begin{aligned}\sigma(x) &= \arg\min_{i\in\mathbb{K}} \dot{V}(x) \\ &= \arg\min_{i\in\mathbb{K}} x'(A_i'P + PA_i)x\end{aligned} \tag{3.18}$$

then this allows us to rewrite (3.17) as

$$\begin{aligned}\dot{V}(x) &= \min_{i\in\mathbb{K}} x'\Big((A_i-\kappa BC)'P + P(A_i-\kappa BC)\Big)x \\ &= \min_{\lambda\in\Lambda} x'\Big((A_\lambda-\kappa BC)'P + P(A_\lambda-\kappa BC)\Big)x \\ &\leq x'\Big((A_{\lambda_0}-\kappa BC)'P + P(A_{\lambda_0}-\kappa BC)\Big)x \end{aligned} \tag{3.19}$$

which holds for any $\lambda_0 \in \Lambda$. The conclusion is that if there exists $P > 0$ such that the inequality

$$(A_{\lambda_0}-\kappa BC)'P + P(A_{\lambda_0}-\kappa BC) < 0 \tag{3.20}$$

is verified for all $\kappa \in (0, \bar{\kappa}]$, then $\dot{V}(x) < 0$, and the origin is a globally asymptotically stable equilibrium point under the first harmonic approximation assumption.

To solve inequality (3.20), it is necessary to define $\bar{\kappa} > 0$ and $\lambda_0 \in \Lambda$. The proposed procedure is to draw the Nyquist plot of the convex combinations $H_\lambda(j\omega) = B(sI - A_\lambda)^{-1}C$ for λ covering the simplex Λ. The value of λ_0 should be chosen to provide $H_{\lambda_0}(j\omega)$ that intersects the real axis in the rightmost point at a frequency $\omega_0 \in \mathbb{R}$. With the intersection defined, we have to set $\bar{\kappa} = -1/H_{\lambda_0}(j\omega_0)$ so that the closed–loop system with $H_{\lambda_0}(s)$ is asymptotically stable for all $\kappa \in (0, \bar{\kappa}]$.

It remains to solve inequality (3.20) in order to determine the matrix $P > 0$ necessary to construct the switching function. Since the inequality (3.20) depends linearly on the unknown parameter κ we split it in two LMIs

$$(A_{\lambda_0}-\kappa_{max} BC)'P + P(A_{\lambda_0}-\kappa_{max} BC) < 0 \tag{3.21}$$

$$(A_{\lambda_0}-\kappa_{min} BC)'P + P(A_{\lambda_0}-\kappa_{min} BC) < 0 \tag{3.22}$$

and notice that by doing this, the inequality of interest holds for every $\kappa \in [\kappa_{min}, \kappa_{max}]$. In fact, multiplying (3.21) by $0 \leq \alpha \leq 1$, multiplying (3.22) by $(1-\alpha)$ and adding all terms, then calling $\kappa = \alpha\kappa_{min} + (1-\alpha)\kappa_{max}$, we obtain

$$(A_{\lambda_0}-\kappa BC)'P + P(A_{\lambda_0}-\kappa BC) < 0 \tag{3.23}$$

With this procedure, one can hope to stabilize the system (3.1)–(3.4). It is important to stress that this procedure is developed upon the approximation of $\phi(e)$ by its describing function, and hence does not guarantee closed–loop stability. In other words, this is just an approximation that validates the describing function method in many systems with practical appealing.

3.3 Illustrative Example

Consider the transfer function already treated in Example 2.1. It may be viewed as a mass–spring–damper system with the addition of an integrator.

The state–space representation is given by

$$\mathcal{G} = \left[\begin{array}{ccc|c} 0 & 1 & 0 & 0 \\ 0 & 0 & 1 & 0 \\ 0 & -k/m & -c/m & 1/m \\ \hline 1 & 0 & 0 & 0 \end{array}\right] \tag{3.24}$$

with $m = 1\ kg$, $c = 7\ N.s/m$ and $k = 10\ N/m$. Let us suppose now that the system is able to provide active damping, and the parameter c may assume the values in the interval defined by $c_{min} = 3\ N.s/m$ and $c_{max} = 7\ N.s/m$, which will be selected by an adequate switching function to be designed. System (3.24) is then unfolded into two subsystems, namely

$$\mathcal{G}_1 = \left[\begin{array}{ccc|c} 0 & 1 & 0 & 0 \\ 0 & 0 & 1 & 0 \\ 0 & -10 & -3 & 1 \\ \hline 1 & 0 & 0 & 0 \end{array}\right] \qquad \mathcal{G}_2 = \left[\begin{array}{ccc|c} 0 & 1 & 0 & 0 \\ 0 & 0 & 1 & 0 \\ 0 & -10 & -7 & 1 \\ \hline 1 & 0 & 0 & 0 \end{array}\right] \tag{3.25}$$

The eigenvalues of A_1 and A_2 show that the first subsystem is under–damped, while the latter one is over–damped. This switched linear system is then fed back with a saturation in the feedback control channel, in the same way as in Example 2.1.

To proceed with the method presented in this section, the Nyquist plot of a convex combination set of systems $H_\lambda(s) = B(sI - A_\lambda)^{-1}C$, with $A_\lambda = \lambda A_1 + (1-\lambda)A_2, \forall \lambda \in [0,1]$. The result is shown in Figure 3.1, where the red lines represent the curves for $\lambda = 0$ and $\lambda = 1$, that is, for each subsystem.

The interest is to find λ_0 such that $H_{\lambda_0}(j\omega)$ intersects the real axis in the rightmost point. This condition is attained by the second subsystem, that is, with $\lambda_0 = 0$. Through examination of the Nyquist plot, we may conclude that $\kappa_{max} < 70$. However, choosing $\kappa_{min} = \kappa_{max}/10$, we observe that the LMIs (3.21)–(3.22) are not feasible for $\kappa_{max} > 23.71$. Matrices $(A_{\lambda_0} - \kappa_{max}BC)$ and $(A_{\lambda_0} - \kappa_{min}BC)$ grow apart and it becomes impossible to solve the LMIs and stabilize the system with the use of a unique Lyapunov function. Further work could be undertaken to explore the possibility of using multiple Lyapunov functions, but this is out of the scope of this report. Let us mention that similar stability analysis can not be performed by the circle criterion in the present case since the open–loop system is not asymptotically stable.

Solving the convex optimization problem

$$\inf_{P>0} \mathrm{Tr}(B'PB) \tag{3.26}$$

subject to the linear matrix inequalities

$$(A_{\lambda_0} - \kappa_{max}BC)'P + P(A_{\lambda_0} - \kappa_{max}BC) + C'C < 0 \tag{3.27}$$

$$(A_{\lambda_0} - \kappa_{min}BC)'P + P(A_{\lambda_0} - \kappa_{min}BC) + C'C < 0 \tag{3.28}$$

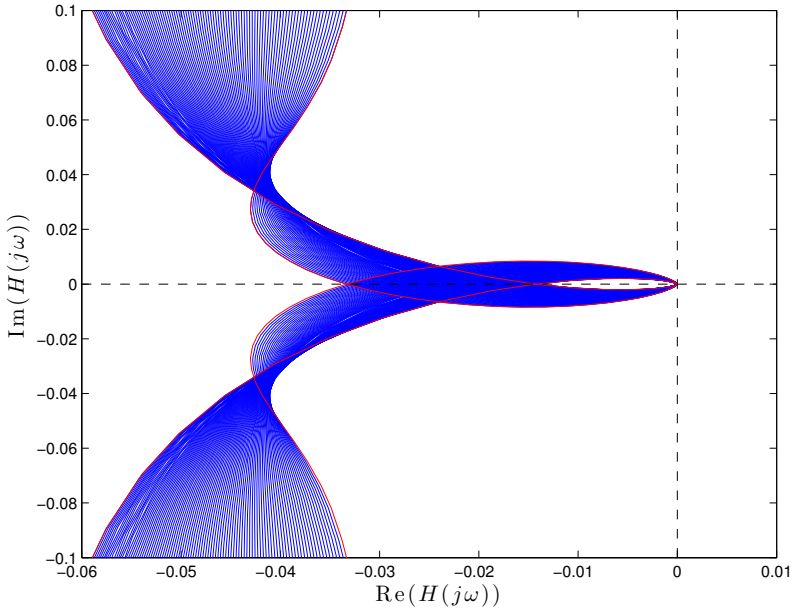

Figure 3.1: Nyquist plot of convex combinations $H_\lambda(j\omega)$

for $\lambda_0 = 0$, $\kappa_{max} = 22$ and $\kappa_{min} = \kappa_{max}/10$ with LMIlab numerical facilities, the result is

$$P = \begin{bmatrix} 13.5299 & 5.9471 & 0.7031 \\ 5.9471 & 6.7309 & 1.0249 \\ 0.7031 & 1.0249 & 0.1617 \end{bmatrix} \tag{3.29}$$

which is used to implement the switching function $\sigma(t) = g(x(t))$. Simulations have been undertaken with this system for a set of initial conditions, $\kappa = h = 20$. The state trajectories are given in Figure 3.2 along with the saturated input $w(t)$. It can be seen that all trajectories are asymptotically stable, even in the presence of the input saturation.

In Figure 3.3, the state trajectories are plot for the initial condition $x_0 = [-2.5 \quad -4.33 \quad 0]'$ along with the switching function $\sigma(t)$ and the saturated input $w(t)$. The vertical dashed lines indicate the instant of time where switching occurs.

These results indicate that the method proposed hereby is able to stabilize Lur'e type systems for which the circle criterion can not be applied. Unfortunately, it does not guarantee stability as the latter does, but the carried out simulations show that the method might be able to stabilize this class of switched linear systems. It is important to stress that the feasibility of (3.21)–(3.22) limits the choice of κ_{max} and κ_{min} to a certain range. A different choice for $\lambda_0 \in \Lambda$ might allow these variables to cover a wider range,

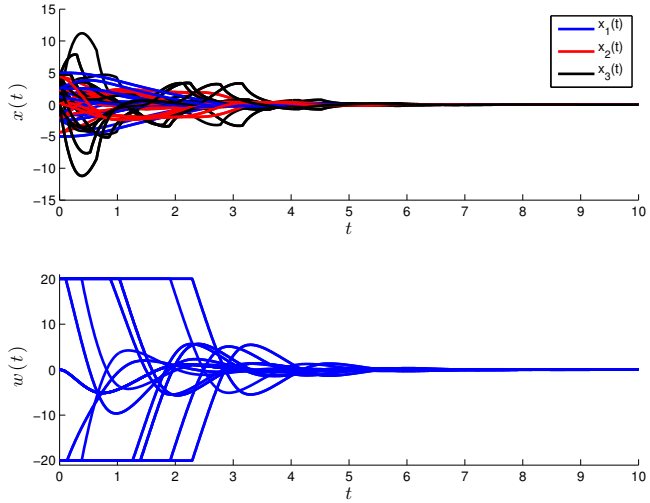

Figure 3.2: State and input trajectories

but at this stage this must be accomplished by trial and error.

The time simulation puts in clear evidence that the designed switching function is very effective for stabilization. The closed–loop system evolves towards the equilibrium point $x_e = 0$ for all considered initial conditions. Moreover, it is evident that the control saturation is active during the beginning of the simulation and the switching rule $\sigma(t) \in \{1, 2\}$ is not uniform (it is not periodic). Indeed, it is state–dependent and activates each subsystem in order to minimize the guaranteed cost

$$\|C\left(sI - \left(A_{\lambda_0} - \kappa BC\right)^{-1} B\right\|_2^2 \leq \mathrm{Tr}(B'PB) \tag{3.30}$$

which is valid for all $\kappa \in [\kappa_{min}, \kappa_{max}]$ and $P > 0$ satisfying the two LMIs indicated before. Since $C'C \geq 0$, these inequalities imply that the previous ones are also satisfied preserving thus asymptotic stability.

Besides stability test, the describing function method is also used to verify the existence of stable limit cycles. By making κ bigger than $\kappa_c = 70$, the system is expected to behave periodically. Time simulations were executed with $\kappa = 1.5\kappa_c = 105$, and the state trajectories along with the switching function and the saturated input are given in Figure 3.4. From the periodic part of the trajectories, we can roughly measure the amplitude and oscillation frequency of the output as being

$$(a_c, \omega_c) \approx (1.5, 3.64) \tag{3.31}$$

which is very close to the values predicted by the describing function method when applied to the second subsystem ($\lambda_0 = 0$) and provided in Example 2.1,

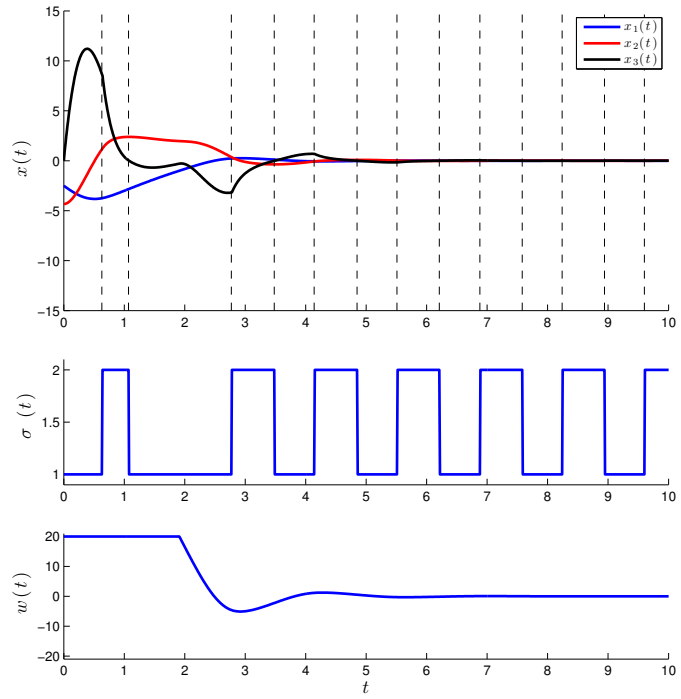

Figure 3.3: State, switching rule and input for a given initial condition

that is $a_c = 1.8074$ and $\omega_c = 3.1623$. These results indicate the existence of a stable limit cycle and confirm the validity of the method.

It is important to stress that we have considered two different saturation functions for simulation purposes. In the two first cases of this Section, we have considered $\kappa = h = 20$ in order to verify that stability was assured by the calculated switching function. On the other hand, in the third case we have used $\kappa = h = 105$ to put in evidence the existence, predicted by the describing function method, of a stable limit cycle that could be compared with the one provided in Example 2.1. It is important to mention again that, in both cases, as we have discussed before, the present method performed very well.

It is important to keep in mind that the first harmonic approximation plays a central role in the present control design problem. As commented before, the parameters $\lambda_0 \in \Lambda$, κ_{min} and κ_{max} are directly determined from the Nyquist plot of the open–loop transfer function and the describing function $L_\phi(a)$ associated to the nonlinearity $\phi(e)$. Nevertheless, if necessary, they must be modified accordingly in order to preserve feasibility of the previous

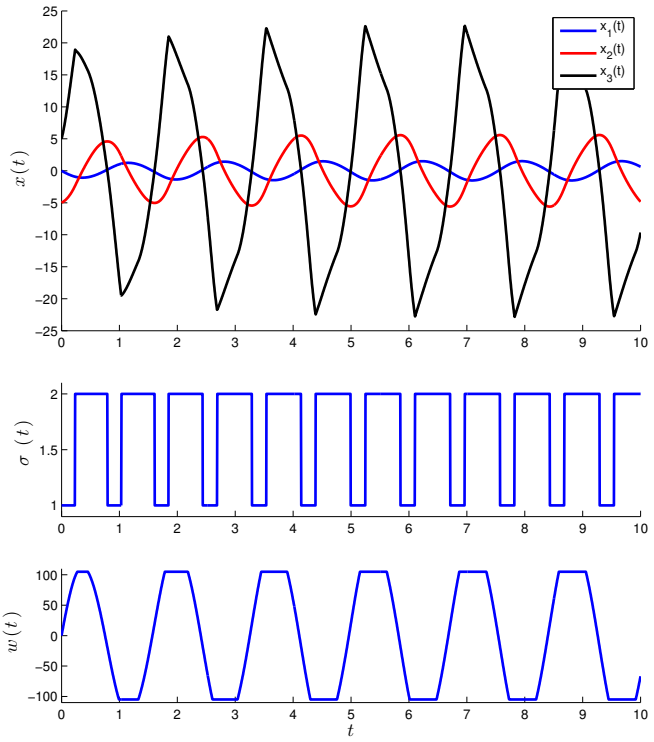

Figure 3.4: Trajectory convergence to a stable limit cycle

LMIs.

Finally, we want to add that matrix $P > 0$ is determined with no big difficulty since the convex programming problem to be dealt with has a linear objective function and two convex constraints expressed by LMIs. Hence, in principle, we do not see any difficulty to handle such class of design problems even if the number of subsystems is greater than two and the state vector is of large dimension.

Chapter 4

Conclusion

In this final undergraduate report, a new method for stability analysis and switching control design of Lur'e type switched systems based on harmonic linearization of the nonlinearity has been developed and successfully tested. In general terms, it consists on the estimation of the maximum closed–loop gain through the Nyquist plot of the best suited subsystem convex combination. The switching rule is derived from a pair of LMIs whose feasibility bounds the closed–loop feasible gains. It is important to notice that this method does not require the linear part of the Lur'e type system be asymptotically stable, an assumption needed for the application of the celebrated circle criterion. The cost of this relaxation (due to the first harmonic approximation) comes in the form of the loss of the sufficient condition for stability.

As deeply discussed, the LMI feasibility problem can be alternatively solved with the use of multiple Lyapunov functions. This would improve the results that could be adopted to cover a wider range of the describing function's critical region. A possible starting point would be to work with the Lyapunov function given in Section 2.2 and try to apply a generalization of Theorem 2.5. These aspects will be considered by the author in the future.

Due to the adopted approximation, the method can not guarantee stability as is the case. The same occurs in the classical application of the first harmonic method to LTI systems. However, as in the classical case, the method applied to switched system stability analysis is very efficient as reveals the simulations of a mass–damper–spring system with an integrator over a wide set of initial conditions. The lack of sufficient conditions for stability is the major drawback of this procedure. Future work might be devoted to try to find a set of sufficient conditions under which the closed–loop system is asymptotically stable. This could mean to limit the set of possible initial conditions or the magnitude of the feedback gain, and hence the nature of the allowed nonlinearity. As a result, an increment in conservatism would be naturally expected.

Bibliography

[1] M. A. Aizerman. On a problem concerning the stability "in the large" of dynamical systems. *Uspekhi Matematich. Nauk*, 4(4):187–188, 1949.

[2] G. S. Deacto. Síntese de controle para sistemas dinâmicos com comutação. M.sc. dissertation, Universidade Estadual de Campinas, 2007.

[3] J. Geromel and G. Deaecto. Stability analysis of lur'e-type switched systems. *Automatic Control, IEEE Transactions on*, PP(99), 2014.

[4] J. Geromel, G. Deaecto, and J. Daafouz. Suboptimal switching control consistency analysis for switched linear systems. *Automatic Control, IEEE Transactions on*, 58(7):1857–1861, July 2013.

[5] J. C. Geromel and P. Colaneri. Stability and stabilization of continuous-time switched linear systems. *SIAM Journal on Control and Optimzation*, 2006.

[6] J. C. Geromel and R. H. Korogui. *Controle Linear de Sistemas Dinâmicos: Teoria, Ensaios Práticos e Exercícios*. Editora Edgard Blucher Ltda., 2011.

[7] W. Kaplan. *Advanced Calculus*, volume 4. Addison-Wesley Reading, MA, 1952.

[8] H. K. Khalil. *Nonlinear systems*. Prentice hall Upper Saddle River, 3rd edition, 2002.

[9] D. Liberzon. *Switching in Systems and Control*. Birkhäuser, 2003.

[10] D. Liberzon and A. S. Morse. Basic problems in stability and design of switched systems. *Control Systems, IEEE*, 19(5):59–70, 1999.

[11] M. Liberzon. Essays on the absolute stability theory. *Automation and remote control*, 67(10):1610–1644, 2006.

[12] X.-M. Sun, W. Wang, G.-P. Liu, and J. Zhao. Stability analysis for linear switched systems with time-varying delay. *Systems, Man, and Cybernetics, Part B: Cybernetics, IEEE Transactions on*, 38(2):528–533, 2008.

Appendix A

MATLAB Codes

This appendix is devoted to presenting the MATLAB scripts used in the simulations presented in Section 3.3. Firstly, the script `Lure.mat` is used to define the problem and solve the LMIs to find the switching rule.

```
% Data for the Illustrative Example

close all; clear all; clc

%% Data
N  = 2;     % Nbr of subsystems
nx = 3;     % Nbr of states

m = 1;      % Mass
cmin = 3;   % Minimum damping
cmax = 7;   % Maximum damping
k = 10;     % Spring stiffness

A{1} = [ 0    1       0;
         0    0       1;
         0 -k/m -cmin/m];

A{2} = [0    1       0;
        0    0       1;
        0 -k/m -cmax/m];

B = [0 0 1/m]';

C = [1 0 0];

D = 0;
```

```
s = tf('s');

max = 1;    % Parameter m of the saturation

%% Nyquist plots
figure
for lambda = 0:10^-2:1
   Alambda = (1-lambda)*A{1} + lambda*A{2};
   [Num,Den] = ss2tf(Alambda,B,C,D,1);
   Hlambda = tf(Num,Den);
   [re,im] = nyquist(Hlambda);
   re = squeeze(re);
   im = squeeze(im);
   plot(re(:),im(:),'b-')
   plot(re(:),-im(:),'b-')
   hold on
end
plot([-0.06 0.01],[0 0],'k--')
plot([0 0],[-0.1 0.1],'k--')
xlim([-0.06 0.01])
ylim([-0.1 0.1])
xlabel('Re$(H(j\omega))$', 'FontSize', 14, 'Interpreter', 'Latex')
ylabel('Im$(H(j\omega))$', 'FontSize', 14, 'Interpreter', 'Latex')


%% Nyquist plot for lambda = lambda0
lambda0 = 0;
Alambda0 = lambda0*A{1} + (1 - lambda0)*A{2};
[Num,Den] = ss2tf(Alambda0,B,C,D,1);
for it = 1:length(Num)
   if(Num(it) < 10^-4)
       Num(it) = 0;
   end
end
for it = 1:length(Den)
   if(Den(it) < 10^-4)
       Den(it) = 0;
   end
end
Hlambda0 = tf(Num,Den);
[re,im] = nyquist(Hlambda0);
re = squeeze(re);
im = squeeze(im);
plot(re(:),im(:),'r-')
```

```
plot(re(:),-im(:),'r-')

%% Definition of kmax and kmin
kmax = 22;
kmin = kmax/10;
kappa = 20;

%% LMIs
setlmis([])

% Definition of P as a single symmetric block
P = lmivar(1,[3 1]); % 1 bloco completo simetrico

% LMI with k = kmin
lmi1 = newlmi;
lmiterm([lmi1 1 1 P], (Alambda0 - kmin*B*C)', 1, 's')
lmiterm([lmi1 1 1 0], C'*C)

% LMI with k = kmax
lmi2 = newlmi;
lmiterm([lmi2 1 1 P], (Alambda0 - kmax*B*C)', 1, 's')
lmiterm([lmi2 1 1 0], C'*C)

% P > 0
lmi3 = newlmi;
lmiterm([-lmi3 1 1 P], 1, 1)

LMIs = getlmis;

% Definition of the objective function
n = decnbr(LMIs); % nbr of decision variables (xi)
c = zeros(n,1);
for j = 1:n
    [Pj] = defcx(LMIs,j,P);
    c(j) = trace(B'*Pj*B);
end

% LMI Resolution
options = [1e-5 0 0 0 0];
[copt,xopt] = mincx(LMIs, c, options)
Popt = dec2mat(LMIs, xopt, P);

% Cell structure for simulation
Q = cell(N);
```

```
for it = 1:N
    Q{it} = A{it}'*Popt + Popt*A{it};
end

save('Lure.mat', 'A', 'Q', 'B', 'C')
```

The switched linear system is then defined as a MATLAB function that will be used during simulation. This function is given by `Lure_sys`.

```
function y = Lure_sys( u )

load('Lure.mat')

w = u(1);   % Input
x = u(2:4); % States

[~, sigma] = min([x'*Q{1}*x x'*Q{2}*x]); % Switching rule

dx = A{sigma}*x + B*w;  % State equations
xi = C*x;               %

y = [xi; sigma; dx];

end
```

The block diagram used for the simulation in SIMULINK is given in Figure A.1.

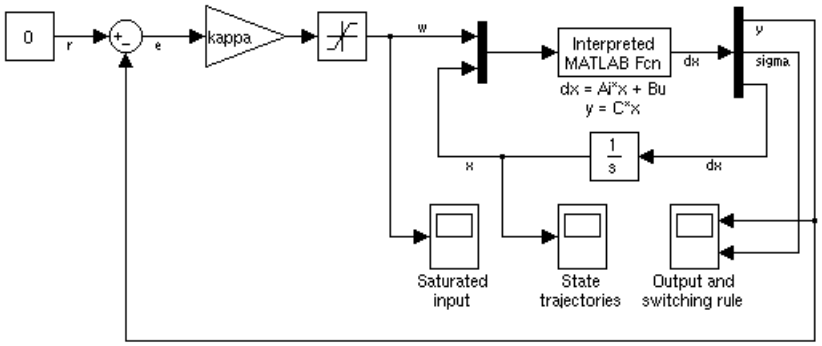

Figure A.1: SIMULINK block diagram